OUKA
Osaka University Knowledge Archive

Title	Low Temperature Synthesis of $SrTiO_3$ Films by Mirror Confinement Type ECR Plasma Sputtering(Physics, Processes, Instruments & Measurements)
Author(s)	Baba, So; Ueno, Toshiyuki; Miyake, Shoji
Citation	Transactions of JWRI. 2000, 29(1), p. 15-20
Version Type	VoR
URL	https://doi.org/10.18910/12210
rights	
Note	

Osaka University Knowledge Archive : OUKA

https://ir.library.osaka-u.ac.jp/

Osaka University

Low Temperature Synthesis of $SrTiO_3$ Films by Mirror Confinement Type ECR Plasma Sputtering †

So BABA *, Toshiyuki UENO * and Shoji MIYAKE **

Abstract

Strontium titanate ($SrTiO_3$) films were synthesized with mirror-confinement-type electron–cyclotron-resonance (ECR) plasma sputtering in a low-pressure Ar gas. The ion flux was found to be controlled by the microwave, while the sputtered particle flux was varied widely by the RF power supply to $SrTiO_3$ target. All as-deposited films were found to be amorphous phases by X-ray diffraction (XRD), and they were crystallized by post-annealing at a temperature of 400 ℃ which is about 200 ℃ lower than the one by conventional RF magnetron sputtering. While post-annealing using 28 GHz millimeter-wave radiation favorably decreased the crystallization temperature further to a value of 300 ℃.

KEY WORDS: (ECR sputtering) (mirror confinement) (RF bias) ($SrTiO_3$) (electromagnetic wave post-annealing)

1. Introduction

Strontium titanate ($SrTiO_3$) has been investigated as a candidate for one of the high dielectric constant materials for dynamic random access memory (DRAM) with higher density than 1 Gbit. This film has been synthesized by several processes such as RF magnetron sputtering,[1)] divergent magnetic field type electron–cyclotron-resonance (ECR) plasma sputtering,[2)] metalorganic chemical vapor deposition (MOCVD),[3)] molecular beam epitaxy (MBE),[4)] pulsed laser deposition (PLD),[5)] and ion beam sputtering[6)]. Among these processes, RF magnetron sputtering is one of the most popular, but high temperatures (above 600 ℃) require synthesis of crystallized $SrTiO_3$ films with high dielectric constant. The dielectric films must usually be synthesized on lower temperature substrates and at a lower post-annealing temperature for application in several devices.

The mirror-confinement-type ECR plasma sputtering[7, 8)] using two magnetic coils can produce a high plasma density with higher ionization at lower pressures compared with a divergent-magnetic-field-type ECR plasma by more efficient plasma confinement. Moreover the energy dispersion of ions extracted from the former plasma is narrower than the latter one and the high energy tail of the ion profile, which sometimes damages films and substrates, is shorter than that of the sputtered neutral atom's energy profile.[8)]

In the preparation of thin films by plasma physical vapor deposition (PVD)/CVD, it is expected that the crystallization and packing density of films can be improved with moderate ion bombardment to the film surface.[9, 10)] Thus, the independent control of ion and sputtered particle flux is important for obtaining highly functional film properties. In the formation of ceramic thin films by ECR plasma sputtering, an RF power has usually been applied to insulator (ceramic) target materials. In this case, the RF energy to the sputtering target may have various influences on the ECR plasma properties, but little research has been performed. Only the influence of the superposition of the RF power to the substrate (not the sputtering target) was studied[11)] in an ECR plasma, which had a low plasma density ($\sim 10^8$ cm^{-3}) around the substrate.

The dielectric films are synthesized frequently as amorphous phases with various PVD processes. Post-annealing has been generally used for the film crystallization with an electric furnace. But for example, pyrochlore phase is easily formed by post-annealing of amorphous $Pb(Zr,Ti)O_3$ (PZT) thin films,[12)] and the diffusion layer, which decreases the effective permittivity, between the film and the substrate is also formed due to the interdiffusion at high temperature.[13)]

In this research, variation of the plasma properties by the RF power supply to the sputtering target materials is clarified experimentally in the mirror-confinement-type

† Received on June 12, 2000
* Graduate Student
** Professor

Transactions of JWRI is published by Joining and Welding Research Institute of Osaka University, Ibaraki, Osaka 567-0047, Japan.

ECR plasma sputtering system. The effects of post-annealing by electromagnetic wave are compared with those by conventional methods for the crystallization of the films.

2. Experimental procedures

Figure 1 shows a schematic diagram of the experimental apparatus. A water cooled stainless-steel vacuum chamber of 135 mm in inner diameter was equipped with a cylindrical water cooled hollow target. The vacuum chamber was evacuated to a base pressure of 1.1×10^{-4} Pa with a turbomolecular pump. The working gas was Ar and the operating pressure was typically 1.3×10^{-2} Pa. The sputtering target of 46 mm in length and 110 mm in inner diameter was located at the center of the mirror, as shown in the figure. In this study, we applied a $SrTiO_3$ (STO) target. An axial distribution of the magnetic flux density (B) is also shown in the figure at a coil current (I_c) of 420 A. The axial position of z=0 cm corresponds to the center of the mirror.

The spatial distribution of the magnetic field can be modified by the use of a yoke which is also depicted in **Fig. 1**. The yoke consists of two 8-mm-thick mild steel plates, each of which was attached to the coil. The mirror ratio is increased by increasing the coil distance or by using the yoke. When the yoke is used, a larger mirror ratio is achieved for the same z_{ECR}, the axial distance of the ECR point from the center of the mirror.[14] In this experiment, the axial distance between the two mirror coils was fixed at 410 mm.

A microwave power of 2.45 GHz was fed through a rectangular TE_{10} mode waveguide, a ferrite isolator with a dummy load, a directional coupler, an E-H tuner, a quarter-wavelength transformer and an E corner, and is then injected into the vacuum chamber. The microwave power was supplied to the vacuum chamber to achieve an ECR discharge at the position of a magnetic field strength of 875 G. The microwave power was varied from 100 to 500 W.

The target was sputtered by an RF power supply with a frequency of 13.56 MHz via a matching network, independent of the microwave power. The RF power was varied from 0 to 200 W. The self-bias negative voltage by the RF power supply was measured using a high-voltage probe (Tektronix P6015A).

An axially movable single probe was used for the measurement of plasma parameters. A low-pass filter (Butterworth type, f_c=50 kHz) was used to reduce RF coupling to the probe.

The optical emission spectra (OES) were measured from the right end of the vacuum chamber, as schematically depicted in **Fig. 1**. The emission was detected through a Czerny-Turner spectrometer (focal length=350 mm, f/4.6, McPherson 2035), and a quartz optical fiber and recorded by an X-Y recorder through a photomultiplier.

STO films were deposited for 60 min at 2.7×10^{-2} Pa in Ar gas. The substrates used were p-type Si(100) wafers with dimensions of 20 mm x 20 mm x 500 μm with electrical resistivities of 0.2 to 0.5Ω cm. The substrate was set at a position 100 mm apart from the center of the mirror along the axis.

As-deposited films were annealed by using both an electric furnace (SH-203D, Motoyama Co.) and a 28 GHz millimeter-wave heating equipment (FGS-10-28, Fuji Denpa Kogyo). Heating and cooling rates were fixed at the conditions of about 20 ℃/min. The soaking time was fixed at 60 min for every post-annealing treatment. The temperature was measured by a K-type thermocouple in contact with the film surface.

The crystal structure of films was identified by X-ray diffraction (XRD) with a Bragg-Brentano θ-2θ geometry on a goniometer (30 kV, 15 mA; MiniFlex, Rigaku Co.) using monochromatic Cu-K_α radiation. The film surface was observed using scanning electron microscopy (SEM) (Superprobe JXA-8600, JEOL Co.) and an electron probe microanalyzer (EPMA) (EDAX PV9900, Philips Co.) was used to determine elemental compositions of the films.

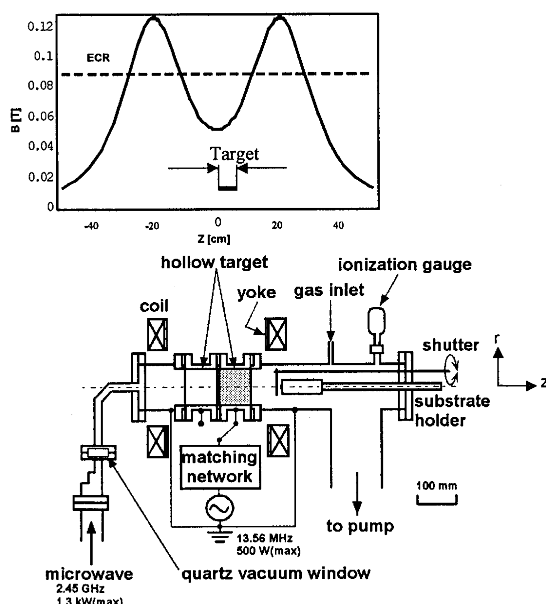

Fig. 1 Schematic diagram of the RF sputtering system enhanced with electron-cyclotron-resonance plasma with mirror confinement.

3. Results and Discussion

3.1 Sputtering properties

Figure 2 shows the axial distribution of electron temperature, T_e, plasma density, N_e and plasma pressure, T_eN_e for microwave power, P_μ=100 W at pressure, p=1.3×10^{-2} Pa without RF power. It is clear that the plasma has a remarkably nonuniform axial distribution. The electron temperature was higher around the center of the plasma column due to the mirror confinement of high energy electrons. On the other hand, the plasma density revealed a maximum value (N_e~1.2×10^{11} cm^{-3}) around the

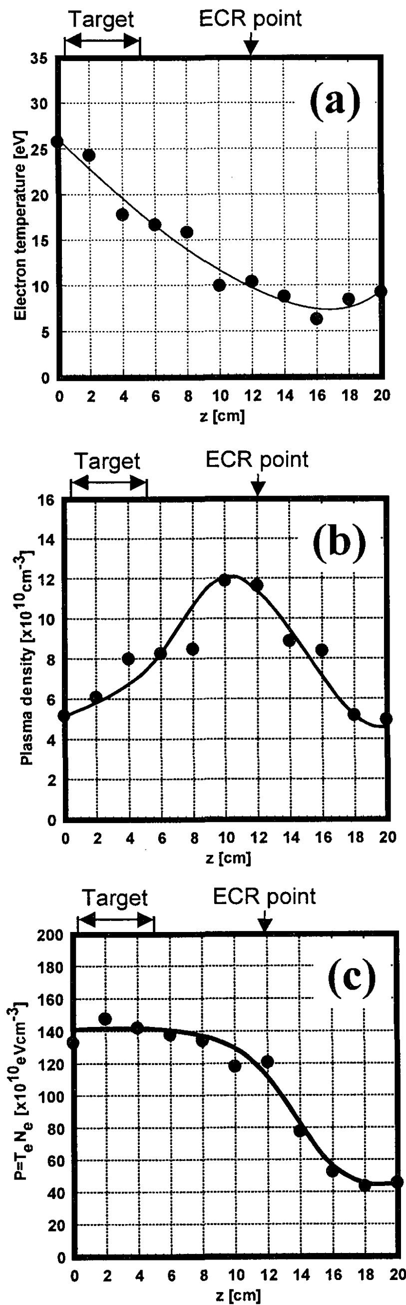

Fig. 2 Axial distribution of (a) electron temperature, (b) plasma density and (c) plasma pressure for P_{rf}=0 W and P_{μ}=100 W.

ECR zone. This result causes the plasma pressure to become nearly constant within the ECR zones, as shown in the figure.

We are interested in the variation of plasma parameters with microwave power around the sputtering target (z=0 cm) and near the substrate (z=12 cm) for the film depositions. **Figure 3** shows the variation of T_e and N_e with P_{μ} at z=0 cm and 12 cm, again at p=1.3x10^{-2} Pa. The electron temperature and plasma density increased with increasing microwave power at both positions, but the variation was stronger at z=0 cm, which is considered

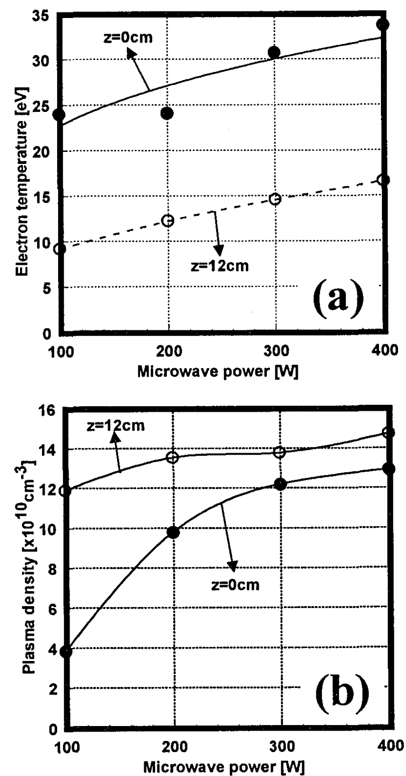

Fig. 3 Variation of (a) electron temperature and (b) plasma density as a function of microwave power for P_{rf}=0 W measured at z=0 cm and at z=12 cm.

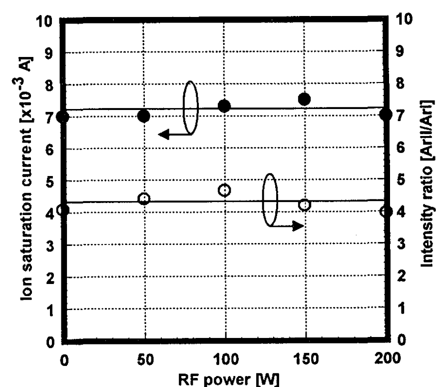

Fig. 4 Variation of the ion saturation current at z=12 cm and the intensity ratio of the ArII line at 476.5 nm to the ArI line at 451.1 nm as a function of RF power for P_{μ}=300 W.

to be due to the efficient electron heating and confinement within the two ECR zones.

Figure 4 shows the variation of the ion saturation current and the intensity ratio of the ArII line emission at 476.5 nm to the ArI line one at 451.1 nm as a function of RF power. The ion saturation current indicates no remarkable variation, even when the RF power is varied widely. The intensity ratio is also negligibly affected by the RF power supply. These results suggests that the

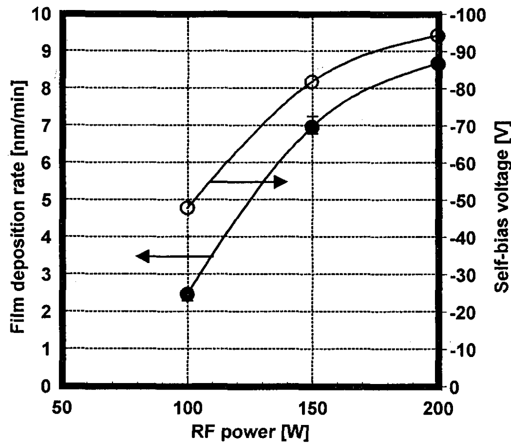

Fig. 5 Variation of the film deposition rate as a function of RF power for P_μ=300 W.

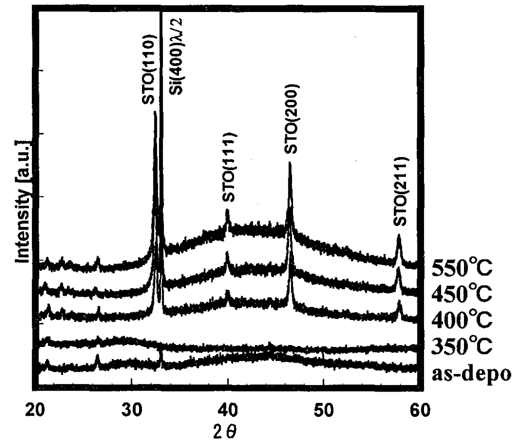

Fig. 6 X-ray diffraction patterns of $SrTiO_3$ films with various post-annealing temperature by electric furnace.

microwave power governs the ionization of Ar gas, that the RF power makes no contribution to additional Ar ionization, and that the ion flux to the substrate can be controlled by microwave power alone, irrespective of the RF power.

$SrTiO_3$ (STO) films were deposited on Si(100) wafers set at z=10 cm. **Figure 5** shows the film deposition rate and the variation of the self-bias negative voltage as a function of RF power at P_μ=300 W. The deposition rate varied significantly with RF power and reached a value of 8.5 nm/min at P_{rf}=200 W. This is a relatively high rate compared with simple RF magnetron sputtering, in which the deposition rate is typically 1~3 nm/min.[1] The film deposition rate is found to show a good correspondence with the variation of the self-bias voltage.

3.2 Film synthesis

All films were deposited without substrate heating, and the mean substrate temperature revealed 140 ℃ during deposition. All as-deposited films were identified to be amorphous phase by XRD. In order to promote the crystallinity of the films, post-annealing was performed by an electric furnace. **Figure 6** shows the XRD patterns of films post-annealed at various temperatures. The $SrTiO_3$ films were crystallized at post-annealing temperature above 400 ℃. This is lower by about 200 ℃ than the one by conventional RF magnetron sputtering.[1] A halo pattern is observed around 40 deg. in 2θ in this figure and this is considered to reveal SiO_2 amorphous phase due to the interdiffusion between the film and the Si substrate.

Figure 7 shows the SEM photographs of film surfaces deposited at various microwave powers and post-annealing temperatures. The thickness of all films was kept constant at about 5000 Å. From the results of plasma properties in this research, an Ar ion flux was increased with increasing microwave power. The ion bombardment, however, does not induce remarkable damage on the as-deposited film surface in the range of $P_\mu \leqq 400$ W regardless of the high-speed synthesis of the films. While the cracks, bubbles and explosion are observed in the post-annealing condition. For the films at P_μ=200 W, the cracks are formed by difference of thermal expansion coefficient between the film and the substrate, while the films deposited at P_μ=300 W and 400 W are not disrupted, probably because the stronger ion bombardment relaxes the thermal stress within the films. For the films at P_μ=400 W, however, many bubbles and hollows are observed. This result can be considered to be caused by the inclusion of a high flux of Ar. **Figure 8** shows the variation of Ar content measured from EPMA of the films with post-annealing temperatures. It is clear that for P_μ=400 W, the Ar intensity decreases with

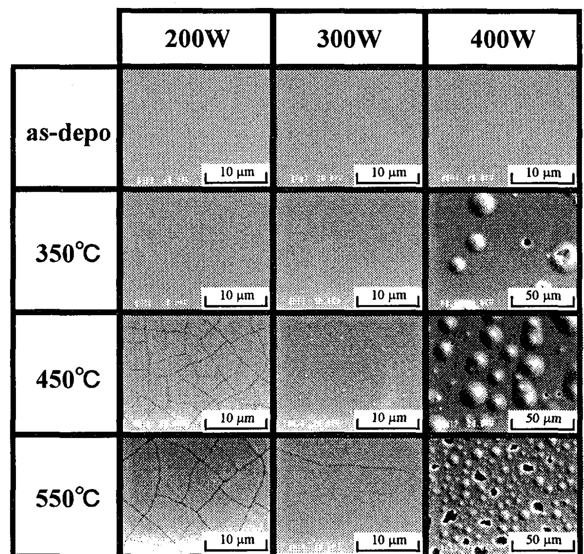

Fig. 7 SEM micrographs of the surface of $SrTiO_3$ films with various post-annealing temperatures for P_μ=200 W, 300 W and 400 W.

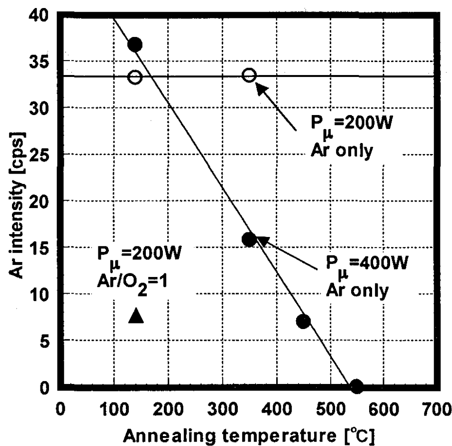

Fig. 8 Variation of the Ar intensity with EPMA as a function of post-annealing temperatures.

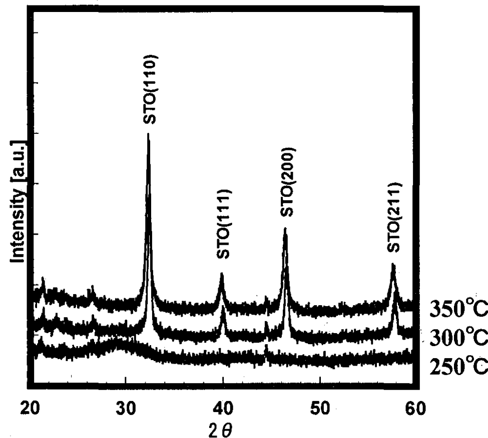

Fig. 9 X-ray diffraction patterns of $SrTiO_3$ films with various post-annealing temperature by electromagnetic wave.

increasing post-annealing temperature. For P_μ=200 W, the intensity does not show any change. A quite low Ar content was obtained from a film synthesized with a plasma of Ar/O_2 mixture. We consider that the bubbles arise from the Ar gases trapped within the films. A large number of bubbles were generated in the films deposited by Ar plasma only during post-annealing, while in the films deposited by Ar/O_2 mixed plasma, decreased. Application of Ar/O_2 plasma is considered to suppresses not only the oxygen vacancies within the perovskite structure but also the damage of the film surface during post-annealing.

Figure 9 shows the XRD patterns of films at various post-annealing temperatures with 28 GHz millimeter-wave radiation. As-deposited amorphous films are crystallized at 400 ℃ with conventional heating, as shown in Fig. 6, while they are crystallized at 300 ℃ with millimeter-wave radiation. Unlike the conventional heating, the halo pattern does not appear in this case around 40 deg. in 2θ. We consider that the microwave causes the dielectric heating of the film and the enhanced transport of atoms and ions for crystallization at a lower temperature.

4. Conclusions

$SrTiO_3$ films were deposited with mirror-confinement-type ECR plasma sputtering in a low-pressure and at a low-temperature. When an RF power was additionally supplied to the sputtering target, the ion saturation current and emission intensity of spectral lines were negligibly influenced. On the other hand, the higher the RF power, the deeper the self-bias negative voltage. These results allow us to suggest that, from the viewpoint of controlling the flux to the substrate, the ion and sputtered particle flux to the substrate can be controlled by microwave and RF powers, respectively. The film deposition rate reached 8.5 nm/min, which was a higher deposition rate than that of RF magnetron sputtering. All the films deposited by the ECR plasma were revealed as amorphous phases, and crystallized at above 400 ℃ with conventional post-annealing. The film surface was smooth regardless of high deposition rate. While the conventional post-annealing at above 450 ℃ caused the formation of SiO_2 amorphous phases between the films and the substrates because of the interdiffusion, and disrupted the film surface at P_μ=200 W by the difference of thermal expansion coefficient between the films and the substrates. Many bubbles were generated in the films deposited by an Ar plasma at higher microwave power and post-annealing temperature. Using 28 GHz millimeter-wave radiation as a post-annealing source the crystallization temperature could be decreased to 300 ℃ and suppress the interdiffusion between the film and the substrate.

Acknowledgements

The authors express their thanks to Dr. Y. Makino and Dr. Y. Setsuhara for their continuous supports and encouragements.

References

1) X. Wang, U. Helmersson, L. D. Madsen, I. P. Ivanov, P. Münger, S. Rudner, B. Hjörvarsson and J. E. Sundgren; J. Vac. Sci. & Technol. A 17 (1999) 564.
2) M. Matsuoka and S. Tohno; J. Vac. Sci. & Technol. A 13 (1995) 2427.
3) Y. B. Hahn and D. O. Kim; J. Vac. Sci. & Technol. A 17 (1999) 1982.
4) Y. Yoneda, T. Okabe, K. Sakaue, H. Terauchi, H. Kasatani and K. Deguchi; J. Appl. Phys. 83 (1998) 2458.
5) M. Tachiki, M. Noda, K. Yamada and T. Kobayashi; J. Appl. Phys. 83 (1998) 5351.
6) Y. Gao, A. H. Mueller, E. A. Irene, O. Auciello, A. Krauss and J. A. Schultz; J. Vac. Sci. & Technol. A 17 (1999) 1880.
7) Z. Y. Ning, Z. P. Luo, Y. C. Shi and Z. X. Ren; Vacuum 43 (1992) 1101.
8) M. Matsuoka and K. Ono; J. Vac. Sci. & Technol.

A 6 (1988) 25.
9) B. Panda, A. Dhar, G. D. Nigam, D. Bhattacharya and S. K. Ray; J. Appl. Phys. 83 (1998) 1114.
10) J. R. Belsick and S. B. Krupanidhi; J. Appl. Phys. 74 (1993) 6851.
11) Y. Ohtsu, Y. Okuno and H. Fujita; Jpn. J. Appl. Phys. 32 (1993) 2873.
12) S. Song, X. Fu, H. Tan, M. Tao, L. Chen, L. Wang and C. Lin; Phys. Stat. Sol. (a), 164 (1997) 779.
13) R.E. Avila, J. V. Caballero, V. M. Fuenzalida and I. Eisele; Thin Solid Films, 348 (1999) 44.
14) M. Mišina, Y. Setsuhara and S. Miyake; J. Vac. Sci. & Technol. A 15 (1997) 1922.